

Melvin–Bonnor and Bertotti–Robinson spacetimes with Baryonic charge

José Barrientos,^{1, 2, 3, *} Fabrizio Canfora,^{4, 5, †} Adolfo Cisterna,^{1, ‡} Keanu Müller,^{6, §} and Anibal Neira^{6, ¶}

¹*Sede Esmeralda, Universidad de Tarapacá, Avenida Luis Emilio Recabarren 2477, Iquique, Chile*

²*Institute of Mathematics of the Czech Academy of Sciences, Žitná 25, 115 67 Praha 1, Czech Republic*

³*Vicerrectoría de Investigación y Postgrado, Universidad de La Serena, La Serena 1700000, Chile*

⁴*Centro de Estudios Científicos (CECs), Avenida Arturo Prat 514, Valdivia, Chile*

⁵*Facultad de Ingeniería, Universidad San Sebastián,*

sede Valdivia, General Lagos 1163, Valdivia 5110693, Chile

⁶*Departamento de Física, Universidad de Concepción, Casilla, 160-C, Concepción, Chile*

Recently, a novel dictionary relating solutions of the Einstein–Scalar–Maxwell theory to solutions of gauged Skyrme–Maxwell–Einstein models in $(3+1)$ dimensions has been established. This development provides a clear and systematic route to constructing new configurations with nontrivial Baryonic charge and magnetic field, leveraging the fact that the Einstein–Scalar–Maxwell system is considerably more tractable, thanks to powerful solution-generating techniques. In this work, we exploit the framework that allows compact sources dressed by scalar fields to be consistently embedded in external electromagnetic backgrounds, and we construct their dual counterparts carrying Baryonic charge in the Skyrme sector. The resulting Baryonic charge is expressed directly in terms of the parameters characterizing the seed spacetime, and a corresponding quantization condition involving these parameters is explicitly derived. Consequently, the mass and the Baryonic charge are not independent parameters. These results provide a closed analytic formula for the black hole mass parameter in terms of the Baryonic charge and the magnetic field. This relation between the mass parameter and the Baryonic charge is linear for large values of the mass, while significant deviations from linearity arise if the mass takes intermediate values.

I. INTRODUCTION

There is little doubt that some of the most important—and at the same time most challenging—open problems in $(3+1)$ -dimensional General Relativity (GR), cosmology, and astrophysics are related to the dynamics of baryonic matter in regions of strong gravity, particularly in the presence of additional ingredients such as stationarity of the compact source or intense electromagnetic fields [1–5]. In such regimes, numerical simulations are not only computationally demanding, but the available analytical tools are also insufficient to construct exact black hole solutions carrying Baryonic charge. Yet the pursuit of analytic solutions is well motivated: as illustrated historically by the discovery of the Schwarzschild and Kerr geometries, exact configurations often reveal novel physical phenomena that would be difficult to uncover by other means.

The technical difficulty in coupling GR to magnetized baryonic matter stems from the simultaneous presence of strong nonlinearities in both GR and in the low-energy limit of QCD. The latter is itself notoriously challenging, since neither lattice QCD nor perturbative methods are reliable in this regime. Nevertheless, the low energy limit of QCD admits an effective description in terms of $(3+1)$ -dimensional gauged Skyrme–Maxwell theory

(GSMT) with $SU(2)$ isospin symmetry [6–12]. Within this framework, GSMT occupies a central role in chiral perturbation theory; see [13–18], where the associated topological charge density is naturally identified with the Baryonic charge density. The development of effective analytical tools in this setting is therefore highly desirable. Such tools would not only complement and inform numerical simulations but would also provide a means to reveal genuinely new phenomena associated with highly magnetized baryonic matter in regimes of strong gravitational fields.

Recently, a mapping relating GSMT and the Einstein–Scalar–Maxwell theory—and, consequently, their respective spectra of exact solutions—has been established [19]. This correspondence is particularly powerful, as it allows one to systematically “transfer” solutions of the Einstein–Scalar–Maxwell system, which carry no Baryonic charge, into the GSMT sector, where they acquire a nontrivial Baryonic charge profile. While the construction of solutions in the Einstein–Scalar–Maxwell theory is itself nontrivial, that framework admits a wide range of well-developed solution-generating techniques. The key advantage of the mapping is that the full effectiveness of these techniques can be directly inherited by the GSMT sector, thereby greatly enlarging the class of analytically accessible configurations with Baryonic charge.

Here, after a concise review of the mapping, we apply it to the case in which the seed spacetimes to be translated into the GSMT sector are Melvin–Bonnor [20–22] and Bertotti–Robinson geometries [23–26], namely configurations describing fully backreacting electromagnetic fields, with or without an embedded compact source. Since the presence of a scalar field is a crucial ingredi-

* jbarrientos@academicos.uta.cl

† fabrizio.canfora@uss.cl

‡ adolfo.cisterna.r@mail.pucv.cl

§ keanumuller2016@udec.cl

¶ aneira2017@udec.cl

ent of the dictionary, we first dress these Melvin–Bonnor and Bertotti–Robinson backgrounds with an appropriate scalar field profile, thereby rendering them suitable seeds. This is achieved through the Eris–Gürses theorem [27], a solution-generating technique valid in the electrovacuum. With these ingredients in place, the baryonic sector can be analyzed in a systematic manner, and the corresponding Baryonic charge can be explicitly computed. Remarkably, a natural quantization condition emerges, relating the Baryonic charge to the parameters characterizing the original seed spacetime.

This work is organized as follows. In Sec. II, we review the main ingredients of the mapping introduced in [19].

Sec. III is devoted to presenting the necessary elements for constructing the seed configurations and to combining them in order to explicitly build the corresponding solutions on the GSMT side, where the associated Baryonic charges are computed. We analyze their behavior and derive the resulting quantization conditions. Finally, in Sec. IV, we present our concluding remarks and outline several directions for future investigation.

II. THE MAPPING

Our starting point is the action of GSMT, which is given by (see [19])

$$S = \int d^4x \sqrt{-g} \left(\frac{1}{4}R - \frac{1}{4}F_{\mu\nu}F^{\mu\nu} + \frac{K}{4}\text{Tr} \left[\Sigma^\mu \Sigma_\mu + \frac{\lambda}{8}B_{\mu\nu}B^{\mu\nu} \right] \right). \quad (2.1)$$

Here, R denotes the Ricci scalar and $K = (f_\pi)^2/4$ defines the Skyrme coupling constant, which is experimentally fixed to $f_\pi \approx 130$ MeV. Note that we adopt the convention $c = 4\pi G = \epsilon_0 = 1$. On the other hand, the pion mass m_π is neglected, as we will focus on configurations with large Baryonic charge; thus, m_π is much smaller

than the characteristic energy scales involved.

As usual, the Einstein field equations are

$$R_{\mu\nu} - \frac{1}{2}g_{\mu\nu}R = 2T_{\mu\nu}, \quad (2.2)$$

where the matter source is given by

$$T_{\mu\nu} = -\frac{K}{2}\text{Tr} \left[\Sigma_\mu \Sigma_\nu - \frac{1}{2}g_{\mu\nu}\Sigma_\sigma\Sigma^\sigma + \frac{\lambda}{4} \left(g^{\alpha\beta}B_{\mu\alpha}B_{\nu\beta} - \frac{1}{4}g_{\mu\nu}B_{\alpha\beta}B^{\alpha\beta} \right) \right] + F_{\mu\alpha}F_\nu^\alpha - \frac{1}{4}F_{\alpha\beta}F^{\alpha\beta}g_{\mu\nu}. \quad (2.3)$$

Here

$$\begin{aligned} \Sigma_\mu &= U^{-1}D_\mu U = \Sigma_\mu^j t_j, & F_{\mu\nu} &= \partial_\mu A_\nu - \partial_\nu A_\mu, \\ B_{\mu\nu} &= [\Sigma_\mu, \Sigma_\nu], & t_j &= i\sigma_j, \end{aligned} \quad (2.4)$$

where σ_i are the Pauli matrices and the $SU(2)$ field U is parametrized by

$$\begin{aligned} U &= 1_{2 \times 2} \cos \alpha + (\sin \alpha) n^j t_j, \\ \vec{n} &= (\sin \Theta \cos \Phi, \sin \Theta \sin \Phi, \cos \Theta), \end{aligned} \quad (2.5)$$

with $1_{2 \times 2}$ denoting the identity 2×2 matrix while $\alpha(x^\mu)$, $\Theta(x^\mu)$ and $\Phi(x^\mu)$ are the three scalar degrees of freedom of the $SU(2)$ -valued Chiral field. On the other hand, the gauge-covariant derivative is

$$D_\mu U = \partial_\mu U + A_\mu [t_3, U]. \quad (2.6)$$

Now, the field equations for the gauge and Skyrme fields are

$$D_\mu \left(\Sigma^\mu + \frac{\lambda}{4}[\Sigma_\nu, B^{\mu\nu}] \right) = 0, \quad \nabla_\mu F^{\mu\nu} = J^\nu, \quad (2.7)$$

being ∇_μ the Levi-Civita covariant derivative, and the current J^μ defined by

$$J^\mu = \frac{K}{2}\text{Tr} \left[\widehat{O} \left(\Sigma^\mu + \frac{\lambda}{4}[\Sigma_\nu, B^{\mu\nu}] \right) \right], \quad (2.8)$$

where $\widehat{O} = U^{-1}t_3U - t_3$.

The Baryonic charge [6–12]

$$Q_B = \frac{1}{24\pi^2} \int_{\mathcal{H}} \rho_B, \quad \rho_B = \rho_{B_1} + \rho_{B_2}, \quad (2.9)$$

with \mathcal{H} being a spacelike hypersurface of dimension three, it is composed of the two distinct topological density terms

$$\rho_{B_1} = \epsilon^{ijk}\text{Tr} \left[(U^{-1}\partial_i U)(U^{-1}\partial_j U)(U^{-1}\partial_k U) \right], \quad (2.10)$$

$$\rho_{B_2} = -3\epsilon^{ijk}\text{Tr} \left[\partial_i [A_j t_3 (U^{-1}\partial_k U + (\partial_k U)U^{-1})] \right], \quad (2.11)$$

where A_j denotes the spatial components of the gauge potential. The term ρ_{B_1} corresponds to the standard

Skyrme contribution, while the second term, ρ_{B_2} , is the so-called Callan–Witten contribution [28].

Keeping these standard technical details in mind, we can formulate a first observation that is crucial for the mapping introduced in [19] and that leads to the desired simplification of the GSMT equations. It is possible to construct a topologically nontrivial ansatz for the Skyrme field for which the Baryonic charge is entirely supported by the Callan–Witten term alone, namely by $\rho_{B_2} \neq 0$, while the standard Skyrme contribution vanishes. In this case, the hadronic and electromagnetic degrees of freedom are drastically simplified, which, in turn, greatly facilitates the construction of gravitating configurations carrying nontrivial Baryonic charge. In mathematical terms, the following ansatz is considered for the $SU(2)$ -valued Skyrme and gauge fields U and A

$$\begin{aligned} \Psi &= \Psi(x^\mu), \quad \Theta = \pi, \quad \Phi = 0 \Rightarrow U = \exp(\Psi t_3), \\ A_\nu &= A_\nu(x^\mu). \end{aligned} \quad (2.12)$$

Following the notation of [19], the Skyrme profile usually denoted by α is here denoted as Ψ .

It is precisely for this ansatz that the Skyrme and Maxwell equations (2.7) simplify to the Klein–Gordon equation and the sourceless Maxwell equations, respectively^{1, 2}

$$\square \Psi = 0, \quad \nabla_\mu F^{\mu\nu} = 0. \quad (2.14)$$

III. BARYONIC MELVIN–BONNOR AND BERTOTTI–ROBINSON SOLUTIONS

As stated above, in order to construct solutions of the fully backreacting GSMT, it is sufficient to first obtain solutions of the Einstein–Scalar–Maxwell theory and then, via the mapping introduced in [19], identify the scalar field that plays the role of the Skyrme degree of freedom. The nontrivial character of the Baryonic density charge crucially relies on the presence of a magnetic field suitably aligned with the gradient of the scalar profile.

Exact solutions endowed with magnetic fields fall into two broad classes: those with localized magnetic charge, such as magnetic monopoles, and those with delocalized magnetic fields, hereafter referred to as external magnetic fields. Our interest lies in the latter case. In particular, we will construct solutions featuring two types of external magnetic fields: Melvin–Bonnor and Bertotti–Robinson.

¹A restriction arises from the low-energy approximation inherent in GSMT. This effective description of QCD ceases to be valid once the energy density associated with the hadronic degrees of freedom becomes too large. In the present context, this translates into imposing

$$|\nabla_\nu \Psi| \lesssim 1 \text{ GeV}. \quad (2.13)$$

²To understand the underlying details of this simplification, we refer to [19].

We begin with the better-known Melvin–Bonnor spacetimes. In electrovacuum and in the absence of compact sources, the Melvin–Bonnor solution describes a static, cylindrically symmetric spacetime representing the backreaction of a magnetic field sharing the same symmetries. It can be interpreted as a magnetic flux tube held together by its own gravitational field. Although this solution can be obtained by direct integration of the field equations, it is more commonly understood as arising from the application of a Harrison transformation [29] to Minkowski spacetime. This approach is advantageous, as direct integration fails in more general settings. The Harrison transformation is a Lie point symmetry of the electrovacuum equations that becomes manifest in the Ernst complex potential formulation [30, 31]. Its generic effect is the generation of electromagnetic fields, whose nature—localized or delocalized—depends on the choice of Killing vector of the seed spacetime used in the transformation.

In the present context, however, the seed spacetime must also support a nontrivial scalar field. Direct integration of the coupled field equations in this case is highly nontrivial. Fortunately, several techniques exist to consistently dress electrovacuum configurations with scalar fields. The most general among them is the Eris–Gürses theorem [27], which has the additional advantage of commuting with charging transformations.

To keep the construction as simple as possible, we will consider Minkowski and Schwarzschild spacetimes as vacuum seeds, dress them with appropriate scalar field profiles, and subsequently magnetize them. These configurations will serve as the starting point for computing the Baryonic charge in the GSMT framework. Here, we only outline the main steps of the construction, referring the reader to [19] for the detailed derivation.

Given any stationary and axisymmetric electrovacuum configuration, the backreaction of a scalar field sharing the same symmetries can be straightforwardly incorporated by means of the Eris–Gürses theorem. To make this procedure explicit, we focus on the static vacuum case—which will be sufficient for our purposes, as we shall consider Minkowski and Schwarzschild spacetimes in what follows—and write the line element in canonical Weyl–Lewis–Papapetrou coordinates $\{t, \rho, z, \varphi\}$, where $-\infty < t < \infty$ and the coordinates $\{\rho, z, \varphi\}$ take their standard cylindrical ranges

$$ds^2 = -e^{2U} dt^2 + e^{-2U} [e^{2\gamma} (d\rho^2 + dz^2) + \rho^2 d\varphi^2], \quad (3.1)$$

with U and γ functions of $\{\rho, z\}$ only. For such a line element, the field equations of the Einstein–Scalar system naturally decouple the backreaction of the scalar. In fact, given a vacuum solution (U, γ) a solution of the Einstein–Scalar theory is given by $(U, \bar{\gamma} = \gamma + \gamma^\Psi, \Psi)$ where the scalar backreaction is found via

$$\gamma_{,\rho}^\Psi = \rho (\Psi_{,\rho}^2 - \Psi_{,z}^2), \quad \gamma_{,z}^\Psi = 2\rho \Psi_{,\rho} \Psi_{,z}, \quad \nabla_{\mathbb{E}^3}^2 \Psi = 0. \quad (3.2)$$

This implies that any vacuum solution can be immersed in a scalar multipolar background determined by the

above quadratures, once a particular solution of the Laplace equation is chosen. The general solution of the Laplace equation contains two distinct types of contributions: asymptotically flat terms, which decay as negative powers of $\mathcal{R} = \sqrt{\rho^2 + z^2}$, and growing terms, which instead behave as positive powers of \mathcal{R} at large distances.

By direct inspection, one finds that within the latter (growing) branch, it is possible to identify configurations that give rise to a nontrivial Baryonic charge. Motivated by this observation, we will restrict our attention to the simplest scalar multipolar background, namely that associated with the first term in the growing sector of the Laplace equation solutions. Taking the Schwarzschild spacetime as the seed (with Minkowski recovered in the massless limit), the corresponding Einstein–Scalar configuration, after transforming back to spherical coordinates, reads [32]

$$ds^2 = -fdt^2 + H \left[\frac{dr^2}{f} + r^2 d\theta^2 \right] + r^2 \sin^2 \theta d\varphi^2, \quad (3.3)$$

with

$$H(r, \theta) = e^{-\Sigma^2 r^2 f \sin^2 \theta}, \quad \Psi(r, \theta) = \Sigma(r - M) \cos \theta, \quad (3.4)$$

and where indeed $f(r) = 1 - \frac{2m}{r}$. With this at hand, the magnetization procedure becomes straightforward. Following [33], where it has been shown at the metric level that, for a given axisymmetric vacuum (or scalar-dressed) solution of the form $ds^2 = g_{ij}dx^i dx^j + g_{\varphi\varphi}d\varphi^2$, its magnetized counterpart is obtained as $ds^2 = \Lambda^2(g_{ij}dx^i dx^j) + g_{\varphi\varphi}d\varphi^2/\Lambda^2$ together with $A = Bg_{\varphi\varphi}d\varphi/2\Lambda$, where $\Lambda = 1 + B^2g_{\varphi\varphi}/4$, we are led to the configuration

$$ds^2 = \Lambda^2 \left(-fdt^2 + H \left[\frac{dr^2}{f} + r^2 d\theta^2 \right] \right) + \frac{r^2 \sin^2 \theta}{\Lambda^2} d\varphi^2, \\ A = -\frac{B r^2 \sin^2 \theta}{2 \Lambda} d\varphi, \quad (3.5)$$

where $\Lambda(r, \theta) = 1 + \frac{B^2}{4}r^2 \sin^2 \theta$. The scalar profile remains unchanged.

Some of the main features of this configuration have already been discussed in [32]. However, for completeness, we highlight here some of its most relevant aspects and complement the discussion with a few interesting limits. First, one can note that the geometry described by the metric (3.5) is of Petrov type I, in close analogy with the Schwarzschild–Melvin solution. The spacetime is not asymptotically flat due to the presence of the electromagnetic field, parametrized by B , which persists at any value of z , because the scalar field gradient becomes aligned with the z -axis at large distances. In addition, the scalar profile grows with the radial coordinate (more precisely, along the original coordinate z), which leads to the appearance of a singularity at infinity. As usual, the central singularity is associated with the compact source at the origin. The singular behavior can be seen explicitly from the expression of the Kretschmann invariant,

both at the origin and at infinity

$$\begin{aligned} R_{\mu\nu\rho\sigma} R^{\mu\nu\rho\sigma} &\underset{r \rightarrow 0}{\sim} \frac{48M^2}{r^6}, \\ R_{\mu\nu\rho\sigma} R^{\mu\nu\rho\sigma} &\underset{r \rightarrow \infty}{\sim} e^{2\Sigma^2 r^2 f \sin^2 \theta}. \end{aligned} \quad (3.6)$$

For $\Sigma = 0$, the solution reduces to the Schwarzschild–Melvin geometry, whereas for $M = 0$ the spacetime remains Petrov type I, unless B or Σ vanish. This background, obtained in the massless limit, will prove useful in what follows, as it allows for a regularization of the Baryonic charge.

The physical intuition is as follows. The Melvin spacetime with the Hadronic profile introduced above is a background that possesses a very large number of Baryons. However, such particles are distributed homogeneously in such a way that no black hole is formed. On the other hand, if extra Baryons are added to the Baryonic–Melvin background (creating a Baryon density peak somewhere), then a black hole may form. This configuration would be a Baryonic black hole in a Melvin background. The important quantity is then the Baryonic charge excess due to the presence of the black hole. In other words, the relevant observable is the difference between the Baryonic charge of the Baryonic–Melvin black hole and the Baryonic charge of the Baryonic–Melvin background (without black hole). Such a quantity encodes the dependence of the black hole mass parameter on the magnetic field and on the Baryonic charge. One of the main results of the present work is that we can compute this dependence analytically.

As it has already been stated in our setup, the Baryonic charge is entirely given by the Callan–Witten term ρ_{B_2} . In the present context ρ_{B_2} reduces to

$$\rho_{B_2} = \epsilon_{ijk} \partial_i A_j \partial_k \Psi, \quad (3.7)$$

which for our configuration (3.5) reads

$$\rho_{B_2} = \frac{\Sigma B(r - M \sin^2 \theta)}{r \Lambda^2}. \quad (3.8)$$

The spatial distribution of the topological charge density ρ_{B_2} can be seen in FIG. 1.

In this case, one observes that along the ρ direction, the density is concentrated near the black hole horizon, with darker blue regions indicating higher density. However, along the z direction, the density increases as one approaches infinity, $|v| = 1$, as reflected by the darker blue shading. This behavior indicates a probable divergence of the topological charge itself.

To plot the Baryonic charge density, we have proceeded as follows: we first change to coordinates

$$r = M + \sqrt{\frac{\rho^2 + z^2 + M^2 + \sqrt{(\rho^2 + z^2 + M^2)^2 - 4M^2 z^2}}{2}}, \\ \cos \theta = \frac{\sqrt{2}z}{\sqrt{\rho^2 + z^2 + M^2 + \sqrt{(\rho^2 + z^2 + M^2)^2 - 4M^2 z^2}}}. \quad (3.9)$$

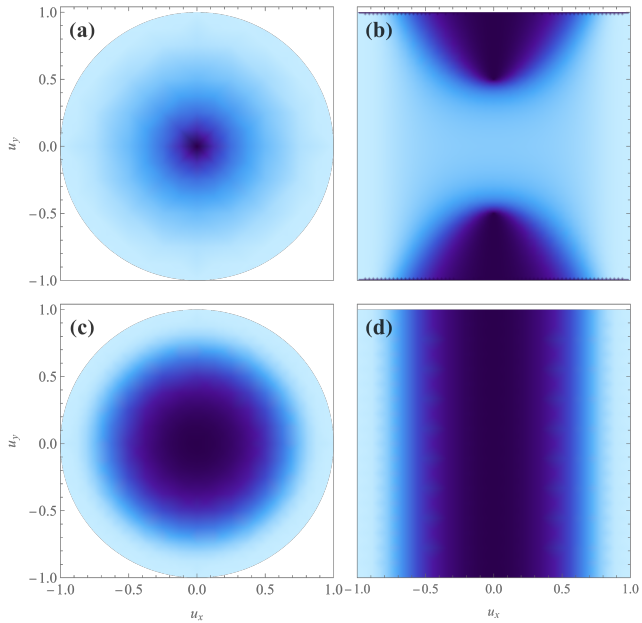


FIG. 1: In panel (a), a $v = \text{const.}$ slice of the Schwarzschild–Melvin configuration is displayed. Panel (b) shows a slice at $u_y = 0$. Panels (c) and (d) present the same sections for the Melvin background solution ($M = 0$). Regions of higher color intensity correspond to a higher Baryonic charge density.

In this chart, the horizon surface is defined as a closed line segment of length $2M$ on the z -axis (with its centre at $z = 0$). One can formally approach it for $|z| \leq M$ by taking $\rho \rightarrow 0$. Then, one can employ the convenient coordinates

$$(u_x, u_y) = \frac{2}{\pi} \arctan \rho (\sin \varphi, \cos \varphi), v = \frac{2}{\pi} \arctan z, \quad (3.10)$$

in which $|z|$ infinity sits at $|v| = 1$ and ρ infinity at $u_x^2 + u_y^2 = 1$. The horizon is again understood as a line segment, now of length $(4/\pi) \arctan M$, on the v axis (with centre at $v = 0$).

The topological Baryonic charge Q_B of the system is obtained by integrating ρ_{B_2} over the volume; it yields

$$Q_B = \int_{\mathcal{H}} \rho_{B_2} = \frac{8\pi\Sigma}{B^2} \left[B(r - 2M) - 4 \frac{(r - M)}{r\sqrt{4 + B^2r^2}} \operatorname{arctanh} \left(\frac{Br}{\sqrt{4 + B^2r^2}} \right) + \frac{1}{\sqrt{1 + B^2M^2}} \operatorname{arctanh} \left(\frac{BM}{\sqrt{1 + B^2M^2}} \right) \right]. \quad (3.11)$$

Notice that this topological charge diverges, confirming our intuition, when one considers the entire range $2M < r < \infty$. This divergence arises because both profiles—the scalar field and the magnetic field component A_φ —are present throughout the whole spacetime and remain constant along the z direction. Note, however, that, as discussed above, this is not surprising at all, since the Baryonic-Melvin background contains a very large number of Baryons. What actually matters is the difference between the Baryonic charge of the Baryonic-Melvin black hole and the Baryonic-Melvin configuration without black hole. This is exactly the same situation as in the analysis of black hole mass in asymptotically AdS spacetime when the mass is measured with respect to the AdS background.

To obtain a finite Baryonic charge, it is therefore necessary to compute the Baryonic charge associated with

the background solution ($M = 0$)

$$Q_B \underset{M=0}{=} \frac{8\pi\Sigma}{B^2} \left[Br - \frac{4}{\sqrt{4 + B^2r^2}} \operatorname{arctanh} \left(\frac{Br}{\sqrt{4 + B^2r^2}} \right) \right]. \quad (3.12)$$

and subtract it from the Baryonic charge corresponding to the configuration in which the compact source is present. The resulting finite Baryonic charge is then given by

$$Q_B = \frac{8\pi\Sigma}{B} \left[\frac{1}{B\sqrt{1 + B^2M^2}} \operatorname{arctanh} \left(\frac{BM}{\sqrt{1 + B^2M^2}} \right) - 2M \right]. \quad (3.13)$$

The corresponding Baryonic density plot is shown in FIG. 2.

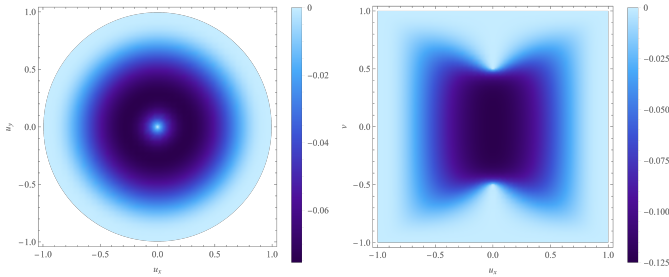


FIG. 2: Baryonic charge density obtained after subtracting the contribution of the Melvin background. The darkest regions indicate where the Baryonic charge is most strongly concentrated.

It is important to emphasize the key implication of the formula above: it provides a relation that determines the black hole mass parameter in terms of its (discrete) Baryonic charge and the magnetic field. In principle, one may invert it to obtain the mass as a function of the topological charge and the magnetic field. Although this inversion cannot be carried out analytically in general, since the resulting equation is transcendental in the mass parameter, it is straightforward to plot the mass as a function of the Baryonic charge for different values of the magnetic field (see FIG. 3).

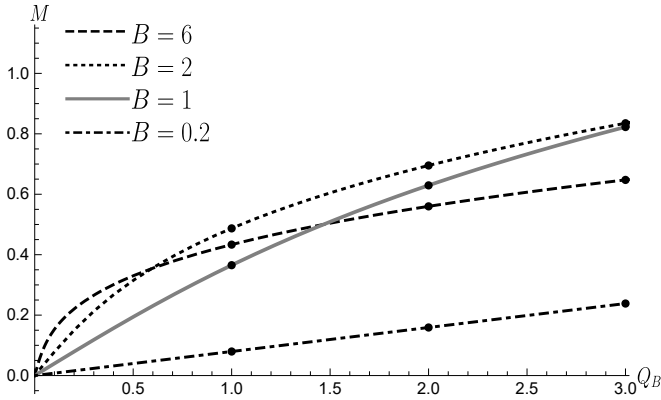


FIG. 3: The mass M as a function of the Baryonic charge Q_B .

The above transcendental equation can be solved analytically in certain limits of interest. When the mass is small, we get

$$M = \frac{1}{4} \frac{\left[(-6Q_B B^2 + 2\sqrt{9B^4 Q_B^2 + 128\pi^2 \Sigma^2}) \right]^{1/3}}{\pi^{1/3} \Sigma^{1/3} B} - \frac{2\pi^{1/3} \Sigma^{1/3}}{B \left[(-6Q_B B^2 + 2\sqrt{9B^4 Q_B^2 + 128\pi^2 \Sigma^2}) \right]^{1/3}}. \quad (3.14)$$

On the other hand, when the mass is very large, the relationship between the mass and the Baryonic charge

becomes linear

$$M = \frac{B}{16\pi\Sigma} Q_B. \quad (3.15)$$

From this analysis, several relevant pieces of information can be extracted. The most immediate observation is that the mass is expected to be proportional to the Baryonic charge, which represents the number of baryons. This behavior is indeed recovered in the large-mass regime.

However, for moderate and small masses, sizeable deviations from this expectation arise. This is precisely the most interesting region, where the interplay between baryonic interactions, the magnetic field, and gravity becomes evident. The plots in FIG. 3 and FIG. 4 show that the largest departures from linearity occur for strong magnetic fields and small Baryonic charge. In this regime, the additional Baryonic charge required to produce a small increase in mass is significantly lower than in the linear regime. Equivalently, the mass grows more rapidly with Baryonic charge than it does at large mass.

Further information can also be extracted, such as generalized susceptibilities, which are related to derivatives of the mass parameter with respect to the magnetic field. A detailed analysis of these quantities will be presented in future work.

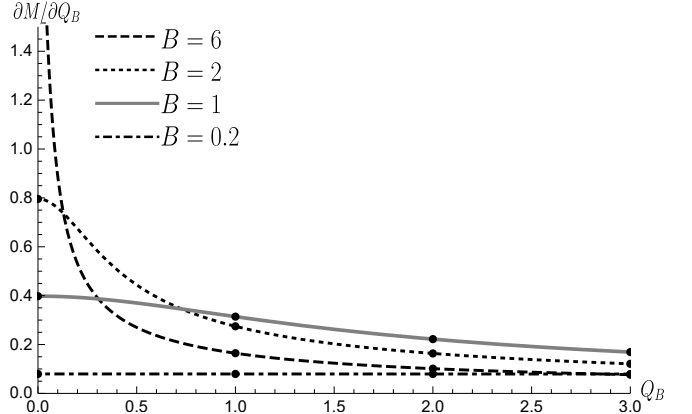


FIG. 4: The behavior of the change of M with respect to Q_B . For small B , $\partial M / \partial Q_B$ becomes constant (dashdotted curve).

A second exact electromagnetic background of interest is the Bertotti–Robinson spacetime [23, 24, 34]. This electrovacuum solution, given by the direct product of two constant-curvature spacetimes, an anti-de Sitter two-dimensional spacetime (AdS_2) and a two-sphere (\mathcal{S}^2), plays an important role not only in the theory of exact solutions of Einstein–Maxwell equations but also in applications to string theory and holography. Embedding a Schwarzschild black hole in the Bertotti–Robinson background again requires the Ernst framework [26], though in this case, the construction relies not on hidden symmetries but rather on direct integration of the Ernst equa-

tions via the so-called monodromy data transform [35–37].

In direct analogy with the Melvin–Bonnor case analyzed above, our starting point is a configuration describing a Schwarzschild black hole embedded in a Bertotti–Robinson magnetic background, which has already been dressed with a scalar field through the application of the Eris–Gürses theorem

$$ds^2 = \frac{1}{\Omega^2} \left(-Q dt^2 + H \left[\frac{dr^2}{Q} + \frac{r^2}{P} d\theta^2 \right] + r^2 P \sin^2 \theta d\varphi^2 \right),$$

$$\Psi = \frac{\Sigma}{2} \ln \left(\frac{r^2 PQ \sin^2 \theta}{\Omega^4} \right), \quad A = \frac{1}{\tilde{b}} (\Omega - r \partial_r \Omega - 1) d\varphi, \quad (3.16)$$

where the backreaction of the scalar field is encoded in

the function

$$H(r, \theta) = \left(\frac{r^2 PQ \sin^2 \theta}{\Omega^4} \right)^{\frac{\Sigma^2}{2}}, \quad (3.17)$$

being

$$Q(r) = \frac{(r(1 - \tilde{b}^2 M^2) - 2M)}{r} (1 + \tilde{b}^2 r^2),$$

$$P(\theta) = 1 + \tilde{b}^2 M^2 \cos^2 \theta,$$

$$\Omega(r, \theta) = \sqrt{1 + r \tilde{b}^2 \left(r - (r(1 - \tilde{b}^2 M^2) - 2M) \cos^2 \theta \right)}. \quad (3.18)$$

Here, \tilde{b} denotes the magnetic field of the Bertotti–Robinson background, while Σ is again the scalar charge.

The Baryonic charge density associated with the Callan–Witten term is given, in this case, by

$$\rho_{B_2} = \frac{\tilde{b} \Sigma \cos \theta}{r \Omega^3} \left[\frac{\tilde{b}^2 M(r - M)(1 + \tilde{b}^2 M r) \cos^2 \theta}{(1 + \tilde{b}^2 r^2)} - \frac{(\tilde{b}^2 [\tilde{b}^2 M^3 r^2 (\tilde{b}^2 M r + 3) - M^2 (M - 6r) - r^2 (3M - r)] + M)}{r Q} \right]. \quad (3.19)$$

The Baryonic charge density shown in [FIG. 5](#) and [FIG. 6](#) resembles the electric charge distribution that arises when a neutral object develops a “charge separation” once an external force acting on the charges is switched on. In the present case, the origin of this effect may be traced back to the magnetic field and its coupling to the hadronic degrees of freedom. Indeed, the place of vanishing Baryonic charge density corresponds to $\cos \theta = 0$ making manifest the similarity with the mechanism of charge separation in polarized media. In such media, the electron cloud is distorted by the external field (which moves the centre of negative charge relative to the positive ones). Moreover, both in the present case and in the case of polarized media, when the “external field” is removed, the charges in the medium generally return to their initial uniform distribution. Here, from the standpoint of the hadronic degrees of freedom, the role of the “external field” is played by the Bertotti–Robinson magnetic field, and hence when such field vanishes, the Baryonic charge density vanishes as well. The key difference with respect to the previous configuration—where a net Baryonic charge is present—is that, in the Melvin black hole case, the hadronic field is an odd function of the polar angle, whereas in the Bertotti–Robinson case, the hadronic profile is even (while in both cases, the gauge potential has the same parity). We will return to this mechanism of Baryonic charge separation in a future publication.

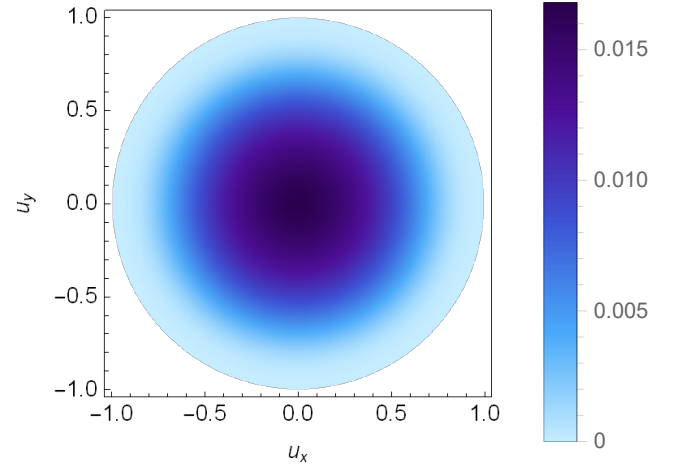


[FIG. 5:](#) A $z = \text{const.}$ slice of ρ_B is displayed, where the charge density is highly concentrated near the event horizon along the ρ -direction and decays monotonically as $\rho \rightarrow \infty$.

IV. CONCLUSIONS AND PERSPECTIVES

In the present manuscript, we have constructed the first analytic example of a black hole carrying Baryonic charge while immersed in a external delocalized magnetic field. These magnetized Baryonic black holes are either asymptotically Melvin–Bonnor or asymptotically

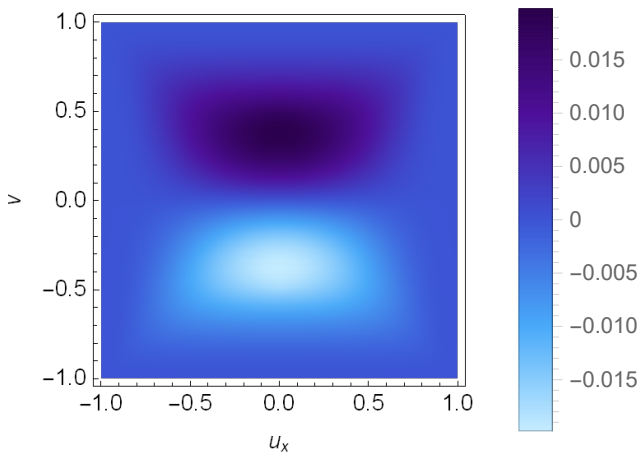


FIG. 6: A $\rho = \text{const.}$ slice shows that the charge density oscillates between positive and negative values, thereby revealing the polarized nature of the configuration.

Bertotti–Robinson. Nicely, we have found that the mass and the Baryonic charge are not independent parameters: we derived a closed analytic expression relating the black hole mass parameter to the (discrete) Baryonic charge and the magnetic field. As this relation is a transcendental equation, we have explicitly analyzed its behavior in relevant limiting regimes, particularly for small masses and moderately large masses.

Our analysis of the Baryonic charge density in the Melvin–Bonnor case shows that the highest density occurs at a finite distance from the horizon and is approximately distributed in a spherical-shell-like region. This is a remarkable outcome for several reasons. First, the Baryonic charge is a discrete topological charge rather than a Noether charge, and to our knowledge, there are no explicit examples in the literature where a black hole mass parameter is expressed directly in terms of a discrete charge. In the present case, the connection between the Baryonic charge and the mass parameter follows from the quantization condition imposed on the Baryonic charge itself. Second, even in flat spacetime and neglecting gravitational backreaction, it is uncommon in strongly interacting systems—particularly at large Bary-

onic charge and in the presence of intense magnetic fields—to obtain an analytic determination of how the total energy depends on the Baryonic charge and the magnetic field.

On the other hand, in the Bertotti–Robinson case, the Baryonic charge density distribution mimics the electric charge distribution of a neutral object polarized by an external agent; indeed, the total net Baryonic charge vanishes. This effect clearly warrants further investigation.

This framework opens several new directions. In particular, it allows the study of the magnetic susceptibilities of the present Baryonic–Melvin black hole through the derivatives of the mass parameter with respect to the magnetic field. This is especially appealing since the magnetic susceptibility encodes key information about the underlying phase structure. This, in turn, opens up the possibility for a detailed exploration of the thermodynamic properties of these backreacting Baryonic configurations.

It would be both interesting and instructive to investigate other exact solutions of the Einstein–Scalar–Maxwell theory that generate nontrivial Baryonic charge configurations, thereby enabling a more systematic study of the phase structure and thermodynamics of these novel systems.

ACKNOWLEDGMENTS

The work of J.B. is supported by FONDECYT Postdoctorado grant 3230596. F.C. has been funded by Fondecyt grants No. 1240048, 1240043, 1240247, and by Grant ANID EXPLORACIÓN 13250014. A.C. is partially supported by FONDECYT grant 1250318. The work of K.M. is funded by Beca Nacional de Doctorado ANID grant No. 21231943. A.N. is supported by ANID–Subdirección de Capital Humano/Doctorado Nacional/2025–21253071. The Centro de Estudios Científicos (CECs) is funded by the Chilean Government through the Centers of Excellence Base Financing Program of ANID. The authors would also like to thank the Conference “Black Hole Physics: Radiation, accelerated spacetimes and beyond” in Licán Ray for providing such an amazing environment in which this work was completed.

[1] A. E. Broderick, M. Prakash, and J. M. Lattimer, Effects of strong magnetic fields in strange baryonic matter, *Phys. Lett. B* **531**, 167 (2002), [arXiv:astro-ph/0111516](https://arxiv.org/abs/astro-ph/0111516).

[2] B. S. Sathyaprakash and B. F. Schutz, Physics, Astrophysics and Cosmology with Gravitational Waves, *Living Rev. Rel.* **12**, 2 (2009), [arXiv:0903.0338 \[gr-qc\]](https://arxiv.org/abs/0903.0338).

[3] D. Giataganas, Baryons under strong magnetic fields or in theories with space-dependent θ -term, *Phys. Rev. D* **98**, 106010 (2018), [arXiv:1805.08245 \[hep-th\]](https://arxiv.org/abs/1805.08245).

[4] C. Watanabe, K. Yanase, and N. Yoshinaga, Searching optimum equations of state of neutron star matter in strong magnetic fields with rotation, *PTEP* **2020**, 103E04 (2020).

[5] J. M. Berryman, S. Gardner, and M. Zakeri, Neutron Stars with Baryon Number Violation, Probing Dark Sectors, *Symmetry* **14**, 518 (2022), [arXiv:2201.02637 \[hep-ph\]](https://arxiv.org/abs/2201.02637).

[6] T. H. R. Skyrme, Particle states of a quantized meson field, *Proc. Roy. Soc. Lond. A* **262**, 237 (1961).

[7] T. H. R. Skyrme, A Nonlinear field theory, *Proc. Roy. Soc. Lond. A* **260**, 127 (1961).

[8] T. H. R. Skyrme, A Unified Field Theory of Mesons and Baryons, *Nucl. Phys.* **31**, 556 (1962).

[9] E. Witten, Current Algebra, Baryons, and Quark Confinement, *Nucl. Phys. B* **223**, 433 (1983).

[10] A. P. Balachandran, V. P. Nair, N. Panchapakesan, and S. G. Rajeev, Low Mass Solitons From Fractional Charges in QCD, *Phys. Rev. D* **28**, 2830 (1983).

[11] G. S. Adkins, C. R. Nappi, and E. Witten, Static Properties of Nucleons in the Skyrme Model, *Nucl. Phys. B* **228**, 552 (1983).

[12] A. P. Balachandran, G. Marmo, B. S. Skagerstam, and A. Stern, *Classical topology and quantum states* (1991).

[13] S. Scherer and M. R. Schindler, *A Primer for Chiral Perturbation Theory*, Vol. 830 (2012).

[14] J. F. Donoghue, E. Golowich, and B. R. Holstein, *Dynamics of the standard model*, Vol. 2 (CUP, 2014).

[15] R. Machleidt and D. R. Entem, Chiral effective field theory and nuclear forces, *Phys. Rept.* **503**, 1 (2011), arXiv:1105.2919 [nucl-th].

[16] J. Gasser and H. Leutwyler, Chiral Perturbation Theory to One Loop, *Annals Phys.* **158**, 142 (1984).

[17] H. Leutwyler, On the foundations of chiral perturbation theory, *Annals Phys.* **235**, 165 (1994), arXiv:hep-ph/9311274.

[18] G. Ecker, Chiral perturbation theory, *Prog. Part. Nucl. Phys.* **35**, 1 (1995), arXiv:hep-ph/9501357.

[19] F. Canfora, A. Neira, and S. H. Oh, Generation of gravitating solutions with Baryonic charge from Einstein-Scalar-Maxwell seeds (2026), arXiv:2601.17864 [gr-qc].

[20] W. B. Bonnor, Static Magnetic Fields in General Relativity, *Proc. Roy. Soc. Lond. A* **67**, 225 (1954).

[21] F. J. Ernst, Black holes in a magnetic universe, *J. Math. Phys.* **17**, 54 (1976).

[22] J. Barrientos, A. Cisterna, I. Kolář, K. Müller, M. Oyarzo, and K. Pallikaris, Mixing “Magnetic” and “Electric” Ehlers–Harrison transformations: the electromagnetic swirling spacetime and novel type I backgrounds, *Eur. Phys. J. C* **84**, 724 (2024), arXiv:2401.02924 [gr-qc].

[23] B. Bertotti, Uniform electromagnetic field in the theory of general relativity, *Phys. Rev.* **116**, 1331 (1959).

[24] I. Robinson, *Bull. Acad. Pol. Sci. Ser. sci. techn.* **7** (1959).

[25] J. Podolsky and H. Ovcharenko, Kerr Black Hole in a Uniform Bertotti-Robinson Magnetic Field: An Exact Solution, *Phys. Rev. Lett.* **135**, 181401 (2025), arXiv:2507.05199 [gr-qc].

[26] G. A. Alekseev and A. A. Garcia, Schwarzschild black hole immersed in a homogeneous electromagnetic field, *Phys. Rev. D* **53**, 1853 (1996).

[27] A. Eris and M. Gurses, Stationary Axially Symmetric Solutions of Einstein-Maxwell Massless Scalar Field Equations, *J. Math. Phys.* **18**, 1303 (1977).

[28] C. G. Callan, Jr. and E. Witten, Monopole Catalysis of Skyrmion Decay, *Nucl. Phys. B* **239**, 161 (1984).

[29] B. Harrison, New solutions of the Einstein-Maxwell equations from old, *J. Math. Phys.* **9**, 1744 (1968).

[30] F. J. Ernst, New formulation of the axially symmetric gravitational field problem, *Phys. Rev.* **167**, 1175 (1968).

[31] F. J. Ernst, New Formulation of the Axially Symmetric Gravitational Field Problem. II, *Phys. Rev.* **168**, 1415 (1968).

[32] V. Cardoso and J. Natário, An exact solution describing a scalar counterpart to the Schwarzschild-Melvin Universe, *Gen. Rel. Grav.* **57**, 138 (2025), arXiv:2410.02851 [gr-qc].

[33] F. Dowker, J. P. Gauntlett, D. A. Kastor, and J. H. Traschen, Pair creation of dilaton black holes, *Phys. Rev. D* **49**, 2909 (1994), arXiv:hep-th/9309075.

[34] T. Levi-Civita, *Rend. Lincei Sci. Fis. Nat.* **26**, 519 (1917).

[35] G. A. Alekseev, *Mat. Inst. Steklova* **176**, 211 (1987).

[36] G. A. Alekseev, General Relativity and Gmuitation 1992, Proceedings of the 13th International Conference, Coroba, Argentina, edited by R. J. Gleiser, C. N. Kozmeh, and O. M. Moreschi (1993).

[37] G. A. Alekseev, *Sov. Phys. Dokl.* **30**, 565 (1985).